

## Numerical simulation of material damage for structural steels S235JR and S355J2G3

Paweł G. Kossakowski\* and Wiktor Wciślik<sup>a</sup>

*Department of Strength of Materials and Concrete Structures, Kielce University of Technology,  
Al. Tysiąclecia Państwa Polskiego 7, 25-314 Kielce, Poland*

*(Received December 12, 2017, Revised January 30, 2018, Accepted February 3, 2018)*

**Abstract.** The paper discusses numerical analysis of tensile notched specimens with the use of Gurson – Tvergaard – Needleman (GTN) material model. The analysis concerned S235JR and S355J2G3 steel grades, subjected to medium stress state triaxiality ratio, amounting 0.739. A complete procedure for FEM model preparation was described, paying special attention to the issue of determining material constants in the GTN model. An example of critical void volume fraction ( $f_c$ ) experimental determination procedure was presented. Finally, the results of numerical analyses were discussed, indicating the differences between steel grades under investigation.

**Keywords:** steel; static tensile tests; Gurson–Tvergaard–Needleman model; determination of model parameters; numerical simulation

### 1. Introduction

Failure processes in structural materials occur in steps and are dependent on the rate of load applied. The failure of brittle materials including concrete or glass is different from that observed in elastic-plastic materials, e.g., structural steels and members (Mahmoud *et al.* 2007, Brnic *et al.* 2013, Brnic and Vukelic 2015, Vukelic and Brnic 2016, Vukelic and Brnic 2017). When steel is used in construction for structural purposes, it is essential to prevent brittle fracture (Boyd 2016), as specified in the European standard EN 1991-1-10: Design of steel structures - Part 1-10: Material toughness and through-thickness properties. Brittle fracture is an extremely dangerous phenomenon mainly because it occurs suddenly and rapidly. It is difficult to predict as there are no macroscale defects to be detected during routine visual inspections required, for instance, for bridges. Recent studies concerning steel bridges have focused on a phenomenon called Constraint Induced Fracture (CIF). This rapid brittle fracture is caused by excessive constraints occurring in structural elements mainly due to the overlapping of welded joints (Connor *et al.* 2007, Hesse *et al.* 2014). It is thus necessary that modern structural steels (grades S235JR and S355J2G3) have high fracture toughness under normal use conditions. Fatigue is another fundamental problem, which is especially important for old structures, i.e., bridges (Kossakowski 2013).

---

\*Corresponding author, Ph.D., D.Sc., E-mail: [kossak@tu.kielce.pl](mailto:kossak@tu.kielce.pl)

<sup>a</sup> Ph.D., Design Engineer, E-mail: [wwcislik@tu.kielce.pl](mailto:wwcislik@tu.kielce.pl)

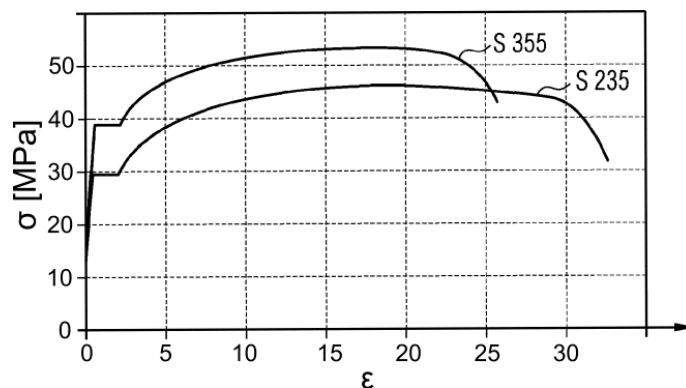


Fig. 1 Typical stress-strain curves for S235JR and S355J2G3 steels basing on (Rasmussen 2011)

The fracture type is dependent on the yielding process, which takes place after the yield point is exceeded (Fig. 1). Metals with polycrystalline structures undergo cracking according to certain patterns. When ductile fracture or shear fracture occurs, the material microstructure is affected. Microdefects in the form of voids are initiated at non-metallic inclusions or second-phase particles present in the material. Void nucleation is also related to the deformation process. The particular stages of ductile fracture can be observed using a round specimen subjected to tensile testing (Fig. 1).

The relationship between the growth of microcracks, defined as the void volume fraction, and the material strength can be determined using the Gurson model for porous materials (Gurson 1977), modified into the Huber-Mises-Hencky (HMH) form. Later, the Gurson model was further transformed, which will be described in the next section.

The Gurson model modified by Tvergaard (1981) and Tvergaard and Needleman (1984), referred to as the Gurson-Tvergaard-Needleman (GTN) model, is commonly mentioned in the literature. It has been implemented in various engineering calculation programs. The GTN method is well suited to model the behaviour (the plastic ranges until failure) of many porous materials, including structural steels commonly used in engineering (Xu *et al.* 2013, Slimane *et al.* 2015), including grades S235JR and S355J2G3 provided that the microstructural parameters and plastic properties of the materials are taken into account (Kossakowski 2014a).

This model is becoming increasingly popular (Oral *et al.* 2010, Cao 2013, Kiran and Khandelwal 2014, Ramazani *et al.* 2014, Malcher *et al.* 2014); it is used in engineering calculations for structures whose material strength is exceeded and where risk of failure is high. In recent years, many attempts have been made to use the GTN model to describe material behaviour under shear conditions (Gatea *et al.* 2017, Smith *et al.* 2013, Cao *et al.* 2014).

The basic problem connected with the use of the GTN model is that generally there is lack of standardized material parameters determined for common structural materials, while in the GTN model there are nine such parameters (Kossakowski 2014b, Kossakowski and Wciślik 2014). The initiation of material failure can be predicted using a parameter called critical void volume fraction  $f_c$ , which determines the moment at which voids form. Its value is generally calculated by analysing the calibration parameters of the GTN structure and comparing the results of the computer modelling with the results obtained during an actual strength test (Teng *et al.* 2014). Another approach is to determine the parameter value physically by examining the material

microstructure at every phase of material failure. In this article, the values of the parameter  $f_c$  are determined experimentally to be further used for the computer modelling of failure of two types of structural steels, i.e., grades S235JR and S355J2G3.

## 2. Specimens used in the investigation

In order to obtain a reference database (for validation of simulation results), a tensile test of the ring notch specimens was carried out (Fig. 2). This kind of specimens allowed to analyze spatial stress state, defined by the stress triaxiality parameter  $\sigma_m/\sigma_e$ , where  $\sigma_m$  is hydrostatic stress and  $\sigma_e$  is equivalent stress. For notched round specimen stress triaxiality depends on its shape and dimensions, or more precisely, on the relations between the specimen diameter and notch radius (depth). Basing on the stress triaxiality defined for these specimens as  $\sigma_m/\sigma_e = 1/3 + \ln[(D/4R) + 1]$ , where  $D$  denotes initial, minimal diameter of the specimen cross-section, and  $R$  is a notch radius, it is possible to obtain different values of  $\sigma_m/\sigma_e$  parameter. For unloaded, smooth tensile specimen without notch, the initial stress triaxiality is  $\sigma_m/\sigma_e = 1/3$ , while for the ring notch specimens  $\sigma_m/\sigma_e > 1/3$ .

The S235JR steel specimens had a notch radius of 3.5 mm, whereas for S355J2G3 steel it was 4 mm. The adopted shape and dimensions of the specimens allowed to obtain the degree of triaxiality amounting 0.739 in the both cases. Figure 2 shows the shape and dimensions of the specimens tested.

Specimens were subjected to static tension. The load was applied by a constant controlled increase in the specimen displacement (elongation) of 2 mm/min. Fig. 3 presents a specimen during the test.

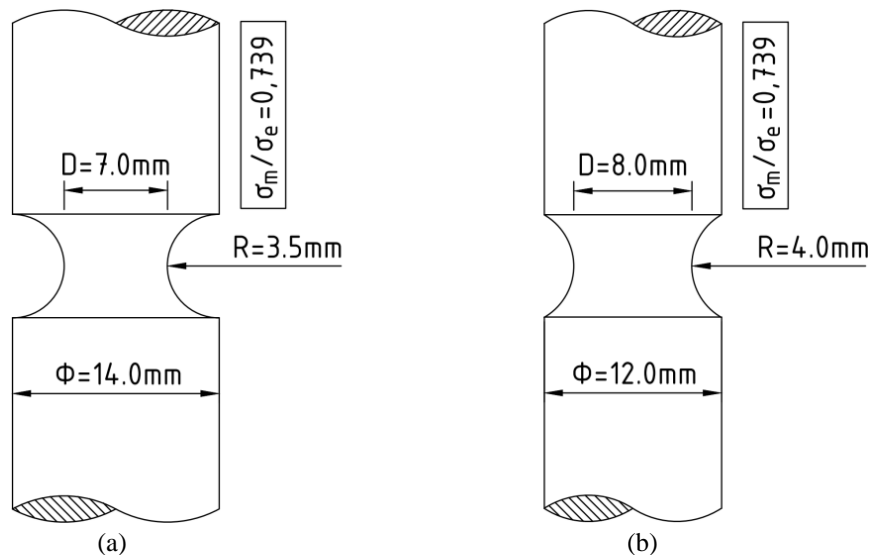


Fig. 2 Shape and dimensions of the analyzed specimens: (a) S235JR steel and (b) S355J2G3 steel



Fig. 3 An exemplary notched specimen under static tension

### **3. Numerical modelling of notched specimen tensile tests**

The primary goal of the present study was to develop a procedure for notched specimen tensile test modelling, taking into account material softening, changes in its microstructure and complex stress states.

The Finite Element Analysis (FEA) was performed using Abaqus software. For each of the analyzed specimens an axisymmetric FEM model was prepared (Fig. 4). Due to specimens symmetry only one quarter was modelled, which corresponds to half of specimens modelled as axisymmetric.

Vertical axis in Fig. 4 can be identified with the loading direction. Axisymmetric type of FEM models and simplification due to their symmetry forced the adoption of appropriate constraints. The adopted support method has prevented the horizontal displacement of the sample axis (X direction), because it is a center of the specimens, which may deform in the vertical direction only (Y direction). Thus, there are no vertical constraints on this boundary. The vertical displacement was blocked in the plane of the notch bottom, which in turn deforms in the horizontal direction (X direction). Due to symmetry of the model vertical deformations are impossible in this area.

Basing on the recommendations given by Xia and Shih (1995) and results obtained by Kossakowski (2012), the FEM mesh size was adopted as 0.25 mm for S235JR and 0.3 mm for S355J2G3 steel. This refers to mesh in the area around the notch (Fig. 4). In the area far from the notch, a larger mesh was adopted.

The load was applied by a constant displacement increase at the top of the model, equal to half of the extension of the extensometer recorded during the experimental study.

In order to enable material softening simulation, GTN material model was adopted. This required the introduction of the actual stretching curve of the material in the uniaxial stress condition. The sought curve was obtained from experimental tensile test performed for unnotched specimens. The basic mechanical parameters of the materials subjected to the analysis are listed in Table 1.

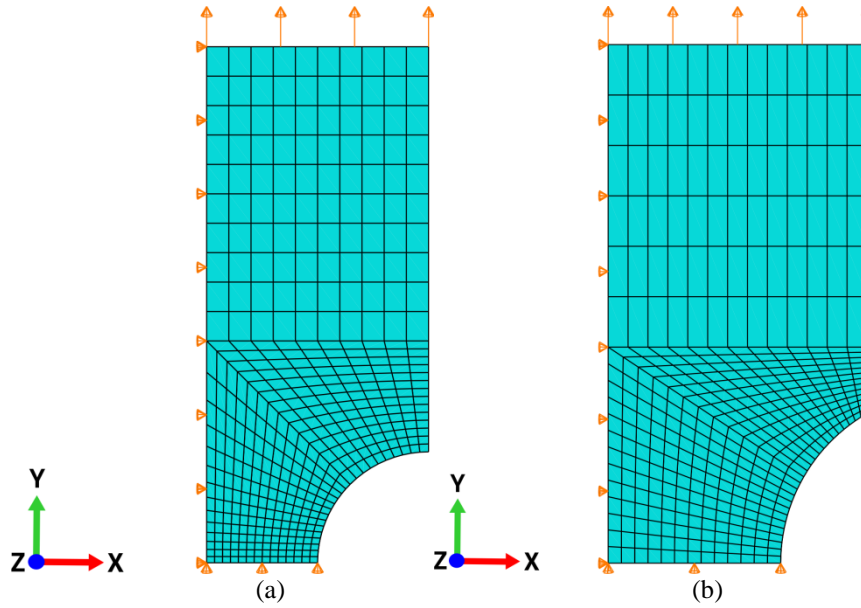


Fig. 4 Numerical models of the specimens: (a) S235JR steel and (b) S355J2G3 steel (drawings in different scales)

Table 1 Mechanical properties of S235JR and S355J2G3 steel determined experimentally

Parameter	S235JR	S355J2G3
Proof strength $R_{0.2}$ [MPa]	318.3	428.0
Tensile strength $R_m$ [MPa]	457.4	683.0
Percentage elongation $A_t$ [%]	33.9	22.7

Since the use of the GTN model requires actual stretching curve determination, the experimental stress – strain curves were approximated by the power equation for elastic-plastic material.

#### 4. GTN model parameters

The GTN model is defined by the following equation (Gurson 1977, Tvergaard 1981, Tvergaard and Needleman 1984)

$$\Phi = \left( \frac{\sigma_e}{R_e} \right)^2 + 2q_1 f^* \cosh \left( \frac{3q_2 \sigma_m}{2R_e} \right) - 1 - q_3 f^{*2} = 0 \quad (1)$$

where:  $\Phi$  – energy of distortion,  $\sigma_e$  – equivalent stress according to the Huber-Mises-Hencky criterion,  $R_e$  – flow stress of the matrix material (yield stress),  $q_1, q_2, q_3$  – Tvergaard's coefficients,  $\sigma_m$  – hydrostatic stress (arithmetic mean of major stresses),  $f^*$  – void volume fraction according to the relations

$$f^* = \begin{cases} f & \text{for } f \leq f_c \\ f_c + \frac{\bar{f}_F - f_c}{f_F - f_c} (f - f_c) & \text{for } f_c < f < f_F \\ \bar{f}_F & \text{for } f \geq f_F \end{cases} \quad (2)$$

where:  $f$  – present void volume fraction,  $f_c$  – void volume fraction at the onset of their coalescence,  $f_F$  – void volume fraction accompanying the specimen failure

$$\bar{f}_F = \frac{q_1 + \sqrt{q_1^2 - q_3}}{q_3} \quad (3)$$

The volume fraction of voids is the sum of the volume resulting from nucleation and the growth of voids. The volume fraction resulting from the nucleation of voids is expressed by the following formula

$$\dot{f}_{nucl} = \frac{f_N}{s_N \sqrt{2\pi}} \exp \left[ -\frac{1}{2} \left( \frac{\varepsilon_{em}^{pl} - \varepsilon_N}{s_N} \right)^2 \right] \dot{\varepsilon}_{em}^{pl} \quad (4)$$

where:  $f_N$  – volume fraction of nucleating particles,  $\varepsilon_N$  – strain necessary to initiate a void,  $s_N$  – standard deviation of void nucleation strain,  $\varepsilon_{em}^{pl}$  – plastic strain of material matrix,  $\dot{\varepsilon}_{em}^{pl}$  – matrix plastic strain rate.

One of the most important issues related to GTN modelling is the adoption of appropriate material parameters. Although the GTN model has been used for many years, no standardized set of its parameters has been developed for the materials most commonly used in technology.

Many attempts to determine GTN parameters can be found in the literature, but they are usually determined basing on matching the simulation and experiment results. Therefore, they are not universal and only constitute a solution to a single specific problem (specimen geometry and load method). However, it should be remembered that some parameters of the GTN model (nucleation strain, critical volume fraction of voids) can be determined in an experimental way.

Table 2 GTN parameters used in simulations

Parameter	Value	
	S235JR steel	S355J2G3 steel
$f_0$	0.0017	0.0009 (Wcislik 2014a)
$f_c$	0.0634 (present study, see paragraph 5)	0.0053 (present study, see paragraph 5)
$f_F$	0.667	0.652 (Wcislik 2014a)
$q_1$	1.90 (Faleskog <i>et al.</i> 1998)	1.80 (Faleskog <i>et al.</i> 1998)
$q_2$	0.81 (Faleskog <i>et al.</i> 1998)	0.82 (Faleskog <i>et al.</i> 1998)
$q_3$	3.61 (Faleskog <i>et al.</i> 1998)	3.24 (Faleskog <i>et al.</i> 1998)
$\varepsilon_N$	0.206 (Kossakowski and Wcislik 2013)	0.255 (Wcislik 2014a)
$f_N$	0.04 (Tvergaard and Needleman 2006)	0.05 (Wcislik 2014a)
$s_N$	0.05	0.05 (Wcislik 2014a)

An important contribution of this work compared to previous works is the application in modelling of the microstructural parameters of the GTN model ( $f_c$ ,  $f_F$  and  $\varepsilon_N$ ) determined in an experimental way. The values of the other GTN parameters have been adopted based on literature data.

The GTN parameters are listed in Table 2.

The method for determining the critical volume fraction of voids ( $f_c$ ) is given in the following paragraph.

## 5. Experimental procedure for critical void volume fraction $f_c$ assessment

The experimental procedure involved a static tensile tests. As previously (paragraph 2), notched specimens (Fig. 2) were used for investigations.

Assuming that critical void volume fraction  $f_c$  is reached at the moment of getting maximum on the force-elongation curve, the microstructure of material strained to that point was investigated (see Fig. 7).

Thus, tensile tests were aborted immediately after the peak force was obtained (Fig. 5). At this time material microstructure was believed to represent critical volume fraction of voids ( $f_c$ ).

The second phase of the experiment included material microstructural analysis. As stress triaxiality ratio was calculated for the specimen center (Fig. 2), it was substantial to analyze material microstructure in this particular region.

For this purpose the strained specimens were cut along their longitudinal axis (Fig. 6). The area where microscopic observations were conducted (specimen centre), is indicated by the circle. In order to prepare for the microscopic examination, the surface obtained was subjected to grinding and polishing. An example of sample prepared for microscopic examinations is in Fig. 7. This made it possible to analyze microstructure of the material subjected to stress triaxiality equal to 0.739.

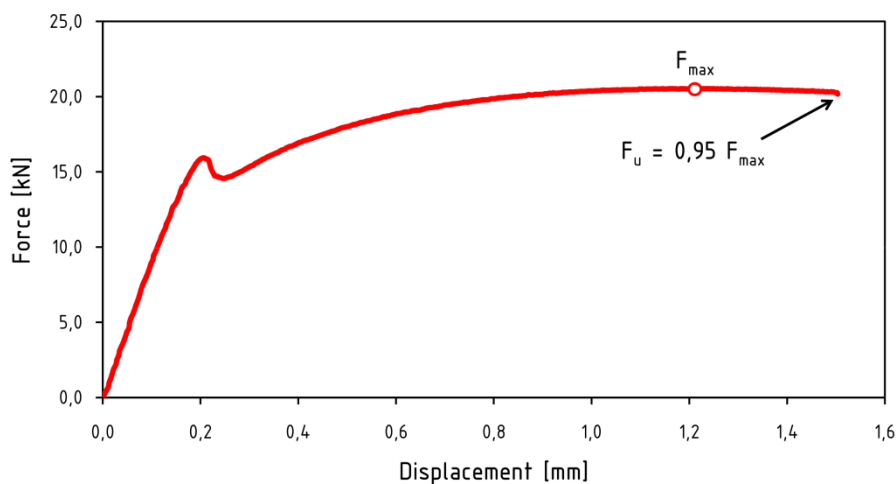


Fig. 5 The moment of interruption of the load associated with obtaining a critical void fraction  $f_c$

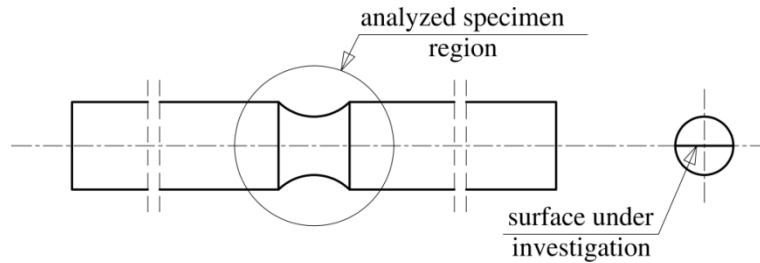


Fig. 6 Part of the notched specimen subjected to microstructural investigations



Fig. 7 An exemplary metallographic sample used to assess the structure of the steel

Microstructural photographs were taken using SEM. Magnification of 1000 x was used. For each sample 60 photos were obtained. An exemplary picture is given in Fig. 8. Grey area represents material matrix, while dark areas indicate inclusions, voids and precipitations. Additional chemical analysis revealed presence of carbides and manganese compounds located in the base material structure. These inclusions are believed to be stress concentrators, initiating development of voids and thus they were taken into account in the calculation of  $f_c$ .

The methodology of the  $f_c$  value estimation included division of photography into a part corresponding to the matrix and material discontinuities and calculation the proportion of discontinuities in the area of the entire photograph. A grayscale – based procedure was developed to perform photograph binarization. The binary version of Fig. 8 is given in Fig. 9. Microstructural discontinuities are clearly visible. Surface fraction of voids and inclusions was calculated using computer software.

Basing on the Chauvenet criterion (Chauvenet 1863), unusual values were rejected.

Taking into account that aerial fraction can be considered as equal to volume fraction (Cavalieri – Hacquet rule), the aerial fractions obtained by using the procedure described above were assumed to be the sought  $f_c$  parameter.

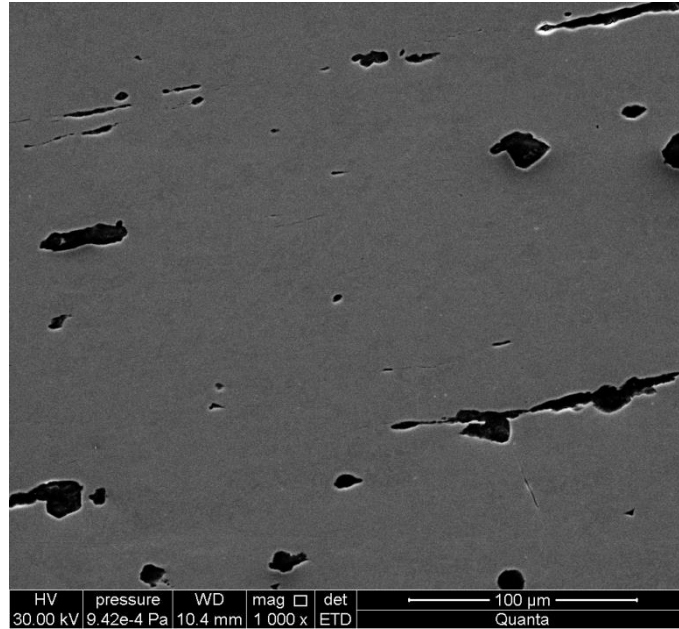


Fig. 8 An exemplary photograph of the deformed steel microstructure used to determine the  $f_c$  value (mag 1000x)



Fig. 9 Figure 8 after binarization

Table 3 Chemical composition of the investigated steel grades

Steel grade	Content of chemical elements [%]						
	C	Mn	Si	P	S	Cr	Ni
S235JR	0.14	0.54	0.17	0.016	0.026	0.12	0.12
S355J2G3	0.19	1.17	0.27	0.015	0.030	0.07	0.10

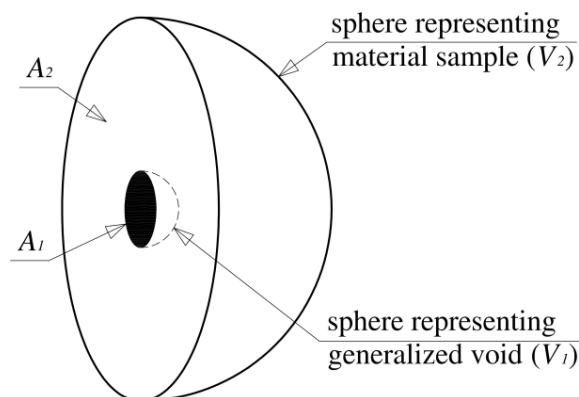


Fig. 10 A scheme for void volume fraction determination, basing on surface fraction of voids

The  $f_c$  values obtained experimentally was 0.0634 (S235JR steel) and 0.0053 (S355J2G3 steel). Authors of the present paper believe that this considerable disparity results from differences in chemical composition (compare Table 3) and ductility of both steel grades.

In both cases, the values of  $f_c$  were definitely higher than the initial porosity  $f_0$  (for the unstrained material – compare Table 2), which indicates a rather intense development of voids in the analyzed load range (it should be remembered that the value of  $f_0$  was also determined as the surface fraction of voids).

The  $f_c$  parameter values determined above were used for computer simulation of the tensile tests of the notched specimens (chapter 6).

Regardless of the assumptions made above, an additional attempt was made to estimate the volume fraction of voids and the second phase particles. For this purpose, based on the above-mentioned surface fraction, a scheme of two concentric spheres was adopted (see Fig.10). The smaller sphere represents the model void, while the larger one represents matrix that surrounds it. It was assumed that the ratio of the cross-sectional area of both spheres is equal to the surface fraction determined in this chapter (0.0634 for S235JR steel and 0.0053 for S355J2G3 steel).

Based on these assumptions, the volume fraction of the smaller sphere (void) in the volume of the material matrix (larger sphere) was calculated. The resultant volume fraction of voids was 0.016 for S235JR steel and 0.0004 for S355J2G3 steel.

Finally, the values of surface fractions, amounting to 0.0634 (S235JR steel) and 0.0053 (S355J2G3 steel), were used in simulation.

## 6. Numerical simulation of damage process of structural steels

Using the previously described numerical models and GTN parameters listed in Table 2, simulations of notched specimens tension was performed for the both steel grades. In the next stage, the simulation and experiment results were compared in the field of force – displacement graphs.

Numerically and experimentally obtained force – displacement force graphs for S235JR steel are presented in Fig. 11.

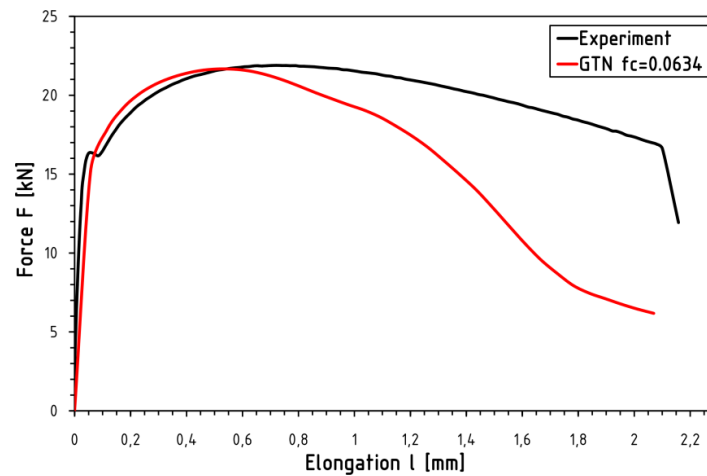


Fig. 11 Experimental and numerical force – displacement curves for S235JR steel

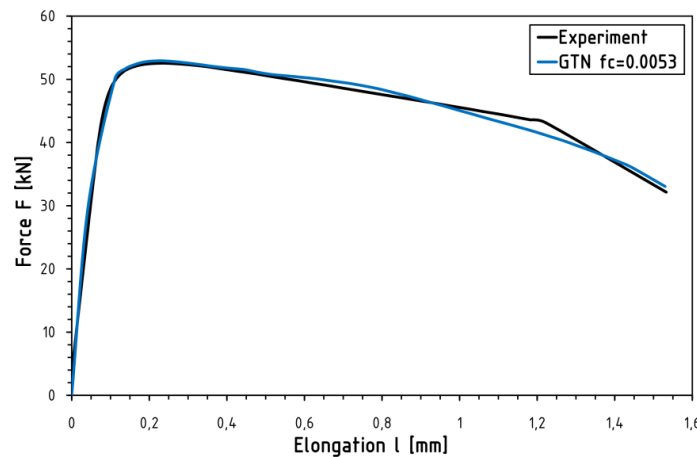


Fig. 12 Experimental and numerical force – displacement curves for S355J2G3 steel

A comparative analysis of both charts indicates their good compatibility in the initial loading phase. The maximum strength obtained experimentally and numerically are almost identical (21.9 kN and 21.67 kN, respectively). It should be noted, however, that they were obtained for different values of elongations (0.721 mm and 0.512 mm). As can be seen, the use of the GTN model allows to describe the softening of the material, but in this case numerically obtained results significantly differ from the results of the experiment. In spite of the fact that in the initial phase of loading the experimental and numerical graphs show good agreement, after exceeding the material strength, the numerically obtained graph falls much earlier, which is related to the underestimation of the loads carried by the specimen and forecasting its premature destruction. The authors of the present work assume that this is due to the relatively high ductility of the steel tested and the assumed parameters of the voids development model (with high strains, it predicts too intensive

growth of voids, which leads to excessive softening of the material).

It is worth stressing, however, that conservative results were obtained, safe from the engineer's point of view.

Analogous results obtained for S355J2G3 steel are shown in Fig. 12. The good consistency of the results of the simulation and experiment is visible. The quality of numerical results is sufficient for practical applications. The maximum force value obtained during the experiment was 52.56 kN, while the result obtained during the simulation was 52.93 kN (difference below 1%).

Significantly larger differences were characterized by the elongation of the specimen at the moment of maximum force. They amounted to 0.243 mm for the experiment and 0.224 mm for the simulation (9% difference).

Also in this case, the use of the GTN model allowed modelling the softening of the material immediately before failure.

## 7. Conclusions

In this work, an attempt was made to simulate the process of tension of specimen with ring notch made of two grades of steel, very commonly used in construction (S235JR and S355J2G3). Specimens with average triaxiality of stress state (0.739) were selected for the analysis. The material model of Gurson – Tvergaard–Needleman (GTN) was used in the modelling.

In many works previously published, model parameters were determined by adjusting simulation and experiment results. In this case, an attempt was made to determine the microstructural parameters of the model experimentally. Particular attention was paid to the critical volume fraction of voids at the moment of their coalescence ( $f_c$ ).

In order to estimate the  $f_c$  value, microstructural investigations of the deformed material were carried out together with a quantitative analysis of the microscopic photographs of the material.

Despite the similar geometry of the specimens and the state of stress prevailing in them, very different values of  $f_c$  were obtained (0.0634 for S235JR steel and 0.0053 for S355J2G3 steel). It is assumed that such significant differences result from differences in the chemical composition and ductility of the tested steels.

Based on the  $f_c$  values obtained experimentally, simulations of previously performed tensile tests were performed. For S235JR steel, a clear discrepancy was observed between simulation and experiment results in the range after material strength was reached. Obtained results were, however, safe, which allows their use in engineering practice. In the case of S355J2G3, good results were obtained.

Regardless of the material analyzed, the conducted research clearly confirmed the suitability of the GTN model to predict softening of the material immediately before failure.

## References

- Boyd, G.M. (2016), “Brittle Fracture in Steel Structures”, Elsevier.
- Brnic, J. et al. (2013), “Analysis of experimental data on the behavior of steel S275JR – Reliability of the modern design”, *Mater. Design*, **47**, 497-504.
- Cao, T.S., Maire, E., Verdu, C., Bobadilla, C., Lasne, P., Montmitonnet, P. and Bouchard, P.O. (2014), “Characterization of ductile damage for a high carbon steel using 3D X-ray micro-tomography and

- mechanical tests – Application to the identification of a shear modified GTN model”, *Comput. Mater. Sci.*, **84**, 175-187.
- Cao, T.S., Montmitonnet, P. and Bouchard, P.O. (2013), “A detailed description of the Gurson–Tvergaard–Needleman model within a mixed velocity–pressure finite element formulation”, *Int. J. Numer. Meth. Eng.*, **96**, 561-583. doi:10.1002/nme.4571
- Chauvenet, W. (1863), *A Manual of Spherical and Practical Astronomy* V. II. Reprint of 1891. 5th Ed., Dover, N.Y., 1960. 474-566.
- Chu, C. and Needleman, A. (1980), “Void nucleation effects in biaxially stretched sheets”, *J. Eng. Mater. Technol.*, **102**, 249-256.
- Connor, R., Kaufmann, E., Fisher, J. and Wright, W. (2007), “Prevention and mitigation strategies to address recent brittle fractures in steel bridges”, *J. Bridge Eng.*, **12**, 164-173.
- Faleskog, J., Gao, X. and Shih, C.F. (1998), “Cell model for nonlinear fracture analysis – I. Micromechanics calibration”, *Int. J. Fracture.*, **89**(4), 355-373.
- Gatea, S., Ou, H., Lu, B. and McCartney, G. (2017), “Modelling of ductile fracture in single point incremental forming using a modified GTN model”, *Eng. Fract. Mech.*, **186**, 59-79.
- Gurson, A.L. (1977), “Continuum theory of ductile rupture by void nucleation and growth. Part I – yield criteria and flow rules for porous ductile materials”, *J. Eng. Mater. Technol.*, **99**, 2-15.
- Hesse, A.A., Atadero, R.A. and Mahmoud, H.N. (2014), “Approach-span failure of the Hoan Bridge as a case study for engineering students and practicing engineers”, *J. Perform. Constr. Fac.*, **28**, 341-348. <https://patentimages.storage.googleapis.com/EP2385245A1/imgf0002.png>
- Kiran, R. and Khandelwal, K. (2014), “Gurson model parameters for ductile fracture simulation in ASTM A992 steels”, *Fatigue Fract. Eng.M.*, **37**, 171-183.
- Koplik, J. and Needleman, A. (1988), “Void growth and coalescence in porous plastic solids”, *Int. J. Solids Struct.*, **24**, 835-853.
- Kossakowski, P. and Wciślik, W. (2013), Effect of stress state triaxiality on the value of void nucleation strain in S235JR steel” (in Polish), *Przegląd Mechaniczny*, **3**, 15-21.
- Kossakowski, P.G. (2013), “Fatigue strength of an over one hundred year old railway bridge”, *Baltic J. Road Bridge Eng.*, **8**(3), 166-173.
- Kossakowski, P.G. (2015), “Microstructural failure criteria for S235JR steel subjected to spatial stress states”, *Arch. Ci. Mech. Eng.*, **15**(1), 195-205.
- Kossakowski, P.G. and Wciślik, W. (2014a), “Effect of critical void volume fraction  $f_F$  on results of ductile fracture simulation for S235JR steel under multi-axial stress states”, *Key Eng. Mater., Fract. Fatigue Mater. Struct.*, **598**, 113-118.
- Kossakowski, P.G. and Wciślik, W. (2014b), “Experimental determination and application of critical void volume fraction  $f_c$  for S235JR steel subjected to multi-axial stress state”, *Recent Adv. Comput. Mech.*, 303-309.
- Kossakowski, P.G. (2014a), “An analysis of the Tvergaard parameters at low initial stress triaxiality for S235JR steel”, *Polish Maritime Res.*, **21**(4), 100-107.
- Kossakowski, P.G. (2014b), “Stress modified critical strain criterion for S235JR steel at low initial stress triaxiality”, *J. Theor. Appl. Mech.*, **52**(4), 995-1006.
- Mahmoud, H.N., Connor, R.J. and Fisher, J.W. (2005), “Finite element investigation of the fracture potential of highly constrained details in steel plate members”, *Comput –Aided Civ Infrastruct. Eng.*, **20**, 383-392.
- Malcher, L., Andrade Pires, F.M. and César de Sá, J.M.A. (2014), “An extended GTN model for ductile fracture under high and low stress triaxiality”, *Int. J. Numer Method. Eng.*, **54**, 193-228.
- Oral, A., Anlas, G. and Lambros, J. (2010), “Determination of Gurson–Tvergaard–Needleman model parameters for failure of a polymeric material”, *Int. J. Damage Mech.*, **21**(1), 3-25.
- Ramazani, A., Abbasi, M., Prah, U. and Bleck, W. (2012), “Failure analysis of DP600 steel during the cross-die test”, *Comput. Mater. Sci.*, **64**, 101-105.
- Rasmussen, A.N. (2011), “Steel tower for a wind turbine”, EP Patent App. EP20, 100, 161, 946.
- Richelsen, A.B. and Tvergaard, V. (1994), “Dilatant plasticity or upper bound estimates for porous ductile solids”, *Acta Metall Mater.*, **42**(8), 2561-2577.

- Slimane, A., Bouchouicha, B., Benguediab, M. and Slimane, S. (2015), "Parametric study of the ductile damage by the Gurson–Tvergaard–Needleman model of structures in carbon steel A48-AP", *J. Mater. Res. Technol.*, **4**(2), 217-223.
- Smith, J., Malhotra, R., Liu, W. and Cao, J. (2013), "Application of a shear-modified GTN model to incremental sheet forming", *Proceedings of the AIP conference*, **1567**, 824-827.
- Teng, B., Wang, W., Liu, Y. and Yuan, S. (2014), "Bursting prediction of hydroforming aluminium alloy tube based on Gurson-Tvergaard-Needleman damage model", *Procedia Eng.*, **81**, 2211-2216.
- Tvergaard, V. (1981), "Influence of voids on shear band instabilities under plane strain conditions", *Int. J. Fract.*, **17**(4), 389-407.
- Tvergaard, V. and Needleman, A. (1984), "Analysis of the cup-cone fracture in a round tensile bar", *Acta Metall Mater.*, **32**(1), 157-169.
- Tvergaard, V. and Needleman, A. (2006), "Three dimensional microstructural effects on plane strain ductile crack growth", *Int. J. Solids Struct.*, **43**, 6165-6179.
- Vukelic, G. and Brnic, J. (2016), "Predicted fracture behavior of shaft steels with improved corrosion resistance", *Metals - Open Access Metallurgy J.*, **6**(2), 40.
- Vukelic, G. and Brnic, J. (2017), "Numerical prediction of fracture behavior for austenitic and martensitic stainless steels", *Int. J. Appl. Mech.*, **9**(4), 1750052 (11p).
- Wciślik, W. (2014a), "Experimental and numerical determination and analysis of Gurson-Tvergaard-Needleman model parameters for S355 steel in complex stress states" (in Polish), Ph.D. Dissertation, Kielce University of Technology, Poland.
- Wciślik, W. (2014b), "Numerical determination of critical void nucleation strain in the Gurson-Tvergaard-Needleman porous material model for low stress state triaxiality ratio", *Proceedings of the 23rd International Conference on Metallurgy and Materials*, Brno, Czech Republic.
- Wciślik, W. (2016), "Experimental determination of critical void volume fraction  $f_F$  for the Gurson Tvergaard Needleman (GTN) model", *Procedia Struct. Integrity*, **2**, 1676-1683.
- Xia, L. and Shih, C.F. (1995), "Ductile crack growth – I. A numerical study using computational cells with microstructurally-based length scales", *J. Mech. Phys. Solids*, **43**(2), 233-259.
- Xu, Y. and Qian, C. (2013), "Application of Gurson–Tvergaard–Needleman constitutive model to the tensile behavior of reinforcing bars with corrosion pits", (Ed., Kreplak L.), *PLoS ONE*, **8**(1), e54368. doi:10.1371/journal.pone.0054368.